not have identical stabilities, they are at least fairly close in energy.

The $\pi$ bond energy of disilene as estimated from the experimental data and obtained from the calculations is much lower than the $\pi$ bond energy in the Si=C double bond that is found to be in the range of 180 ± 20 kJ/mol.[16,32-35] Such a result is not unreasonable because as was shown theoretically,[35] the rather large value for the Si=C double bond is caused mainly by bond polarization, an effect which cannot operate in the case of disilene.

**Acknowledgment.** We thank Mr. W. Sonntag for able technical assistance.

**Registry No.** $SiH_4$, 7803-62-5; $Si_2H_6$, 1590-87-0; $Si_3H_8$, 7783-26-8; $Si_4H_{10}$, 7783-29-1; $H_2SiSiH_2$, 15435-77-5.

---

(32) Potzinger, P.; Reimann, B.; Roy, R. S. *Ber. Bunsenges. Phys. Chem.* **1981**, *85*, 1119–1122.
(33) Davidson, I. M. T.; Potzinger, P.; Reimann, B. *Ber. Bunsenges. Phys. Chem.* **1982**, *86*, 13–19.
(34) Wood, I. T. Ph.D. Thesis, University of Leicester, 1983.
(35) Ahlrichs, R.; Heinzmann, R. *J. Am. Chem. Soc.* **1977**, *99*, 7452–7456.

---

# Stereochemistry of the Insertion of Manganese into Si–H and Ge–H Bonds. Complexes Containing a Two-Electron, Three-Center Mn•••H•••Si (or Ge) Interaction

Francis Carré, Ernesto Colomer, Robert J. P. Corriu,* and André Vioux

*Laboratoire des Organométalliques, Laboratoire Associé au C.N.R.S. No. 349, Université des Sciences et Techniques du Languedoc, Place Eugène Bataillon, 34060 Montpellier Cedex, France*

*Received December 28, 1983*

A crystallographic study of the complex (−)-($\eta^5$-$CH_3C_5H_4$)$(CO)_2$(1-NpPhMeSi)(H)Mn (1, 1-Np = 1-$C_{10}H_7$, Ph = $C_6H_5$, Me = $CH_3$) reveals that the oxidative addition of (+)-1-NpPhMeSiH on methylcymantrene takes place with retention of configuration at silicon. The germyl complexes ($\eta^5$-$CH_3C_5H_4$)$(CO)_2$($R_3$Ge)(H)Mn are prepared either by oxidative addition of $R_3GeH$ (R = Ph) on ($\eta^5$-$CH_3C_5H_4$)$(CO)_3$Mn or by protonation of the related anions $[(\eta^5\text{-}CH_3C_5H_4)(CO)_2(R_3Ge)Mn]^-$ ($R_3$ = $Ph_3$, 1-NpPhMe, $Cl_3$). Only the cis isomers are obtained. Complex 2 (R = Ph) exhibits a higher acidity than the silyl analogue. This acidity is close to that of HCl. However both 1 and 2 undergo easy elimination of $R_3SiH$ or $R_3GeH$ when treated with $PPh_3$. The Mn–Ge bond is cleaved by $H_2O$, $CH_3OH$, $Cl_2$, and $CCl_4$; this behavior contrasts with that of 1 since $Cl_2$ or $CCl_4$ lead to elimination. These observations are in agreement with a two-electron, three-center bond between manganese, silicon (or germanium), and hydrogen.

## Introduction

Oxidative addition of a Si–H bond to a transition-metal center is a key step in catalytic hydrosilylation reactions.[1,2] The addition–elimination process is a fast equilibrium.[3] This process takes place with retention of configuration (RN) at silicon, as deduced from the catalytic SiH/SiD exchange[4,5] rather than with a double inversion (INV) that seems less probable since the Si–H bond is always displaced with retention of configuration (Scheme I).

The mechanism of the oxidative addition of a Si–H bond to a transition metal has been suggested to proceed via a three-center transition state.[6-8] In order to understand thoroughly the

bonding, we have studied the complexes formed by oxidative addition of silanes to ($\eta^5$-methylcyclopentadienyl)tricarbonylmanganese, first described by Graham et al.[9] (Scheme II).

Scheme I

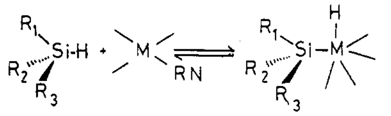

Scheme II

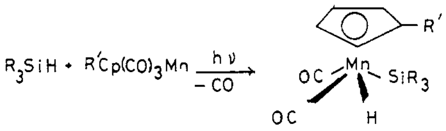

R'=$CH_3$,H; R=Cl,$C_6H_5$; Cp=$\eta^5C_5H_4$

Scheme III

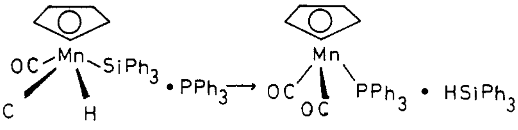

Indeed, X-ray structure determinations are in agreement with a close contact (≤2.0 Å) between the silicon and the

---

(1) Lukevics, E.; Belyakova, Z. V.; Pomerantseva, M. G.; Voronkov, M. G. J. Organomet. Chem. Library **1975**, *5*, 1 and references therein.
(2) Speier, J. L. *Adv. Organomet. Chem.* **1979**, *17*, 407 and references therein.
(3) Corriu, R. J. P.; Moreau, J. J. E. *Tetrahedron Lett.* **1973**, *45*, 4469; *J. Organomet. Chem.* **1976**, *120*, 337.
(4) Sommer, L. H.; Michael, K. W.; Fujimoto, H. *J. Am. Chem. Soc.* **1967**, *89*, 1519.
(5) Sommer, L. H.; Lyons, J. E.; Fujimoto, H. *J. Am. Chem. Soc.* **1969** *91*, 7051.
(6) Eaborn, C.; Tune, D. J.; Walton, D. R. M. *J. Chem. Soc., Dalton Trans.* **1973**, 2255.
(7) Harrod, J. F.; Smith, C. A. *J. Am. Chem. Soc.* **1970**, *92*, 2699.
(8) Harrod, J. F.; Smith, C. A., Than, K. A. *J. Am. Chem. Soc.* **1972**, *94*, 8321.
(9) Jetz, W.; Graham, W. A. G. *Inorg. Chem.* **1971**, *10*, 4.

0276-7333/84/2303-1272$01.50/0 © 1984 American Chemical Society

Scheme IV

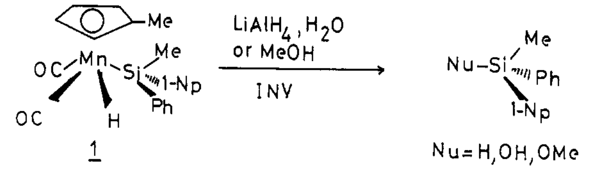

Scheme V

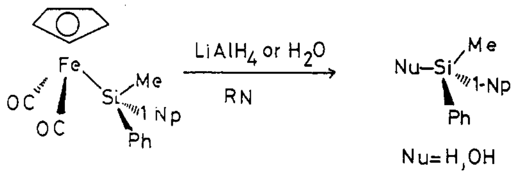

hydrogen ligands.[10] Graham related this structural feature with the great ability of these compounds to undergo silane replacement by a phosphine[11] (Scheme III). In the parent rhenium compounds, the X-ray study showed a longer Si–H distance (~2.2 Å),[12] which seems to be associated with a lower ability for the elimination of silane.[13]

Our previous works[14-16] concerning the spectral and chemical properties of these manganese complexes led us to assume the existence of a three-center, two-electron bond in the Mn–Si–H triangle.

Indeed, the high $^2J$(Si–H) coupling constants observed for this kind of complex are intermediate between $^1J$(Si–H) and $^2J$(Si–H) and are satisfactorily explained by this structure. A later neutron diffraction study of a parent compound[17] supported our assumption.

It is interesting to notice that the expected diastereoisomers (due to chirality at both silicon and manganese atoms) were not observed. Even $^1$H NMR studies at low temperature did not indicate the presence of such isomers.

The well-established equilibrium between 18- and 16-electron species that explains the prototropy between Mn–H and Si–H protons cannot be invoked to explain a fast interconversion of the diastereoisomers, since this equilibrium is slow at the NMR time scale (indeed, these protons show different resonances and are coupled at room temperature). However, a three-center-bond structure could exclude chirality at manganese since the manganese atom could then be considered surrounded by four ligands instead of five.

Another of our main arguments is provided by the stereochemical behavior of the optically active complex 1 (Scheme IV) prepared from optically active (+)-1-NpPhMeSiH (1-Np = 1-naphthyl).[14] Nucleophilic substitutions at silicon occur with inversion of configuration. This stereochemistry is not expected since retention has been observed in the related silyliron complex ($\eta^5$-$C_5H_5$)(CO)$_2$($R_3Si^*$)Fe[18] (Scheme V). We assign this dramatic change of stereochemistry to the presence of the hydrogen ligand. Indeed, the pseudopentacoordination resulting from the hydrogen bridge prevents the frontside attack of the nucleophile, directing the reaction toward the backside attack, corresponding to inversion of configuration.[19]

Scheme VI

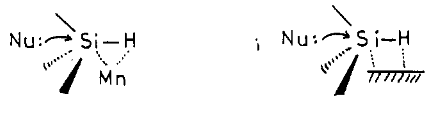

A possible parallel can be drawn with the cleavage reactions of the Si–H bond with oxygen-containing nucleophiles. Without catalyst the reaction proceeds stereospecifically with retention of configuration at silicon.[20]

$$R_3Si^*H + KOH \rightarrow R_3Si^*OK \xrightarrow{H_2O} R_3Si^*OH \quad RN\ 95\%$$

In contrast a poor stereospecificity is observed with homogeneous catalysts.[21]

$$R_3Si^*H + ROH \xrightarrow{\text{Wilkinson's catalyst}} R_3Si^*OR \quad RN \text{ or } INV$$

However the stereochemistry is displaced toward inversion of configuration in the presence of heterogeneous catalysts.[22]

$$R_3Si^*H + ROH \xrightarrow[-H_2]{\text{Raney Ni}} R_3Si^*OR \quad INV\ 100\%$$

The activation process in heterogeneous catalysis probably arises from an adsorption of the Si–H bond on the metal surface, followed by a backside attack of the nucleophile (Scheme VI). It is noteworthy that this adsorption intermediate can be related to the soluble manganese complexes that undergo nucleophilic substitutions with the same stereochemistry.

The present work was undertaken with two purposes: (i) The need to support our stereochemical argumentation by an X-ray determination of the absolute configuration around the Si atom in the optically active complex 1. Indeed the stereochemistry of the nucleophilic cleavage of the Mn–Si bond was based on the assumption that the oxidative addition of the starting silane to manganese took place with retention (Scheme I). (ii) The interest to extend our study to hydrogermylation processes by comparing the silylmanganese complexes to the germylmanganese analogues. The comparison between the optically active compounds offered the most interest. Thus, we have investigated the synthesis of one optically active germyl complex.

## Experimental Section

All reactions were carried out under nitrogen, using a vacuum line, in Schlenk tubes. Solvents were dried, distilled, and deoxygenated ($\eta^5$-$CH_3C_5H_4$)(CO)$_3$Mn was purchased from Strem Chemicals Inc. Other starting materials were prepared by literature methods: $Ph_3GeH$,[23] $Ph_3GeLi$,[24] (*R*)-(+)-MePh-1-NpGeH,[25] (*R*)-MePh-1-NpGeLi,[26] and $Me_4NGeCl_3$.[27] Photo-

---

[10] Cowie, M.; Bennett, M. J. *Inorg. Chem.* **1977**, *16*, 2325 and references therein.

[11] Hart-Davis, A. J.; Graham, W. A. G. *J. Am. Chem. Soc.* **1971**, *93*, 4388.

[12] Smith, R. A.; Bennett, M. J. *Acta Crystallogr., Sect. B* **1977**, *B33*, 1113.

[13] Dong, D. F.; Hoyano, J. K.; Graham, W. A. G. *Can. J. Chem.* **1981**, *59*, 1455.

[14] Colomer, E.; Corriu, R.; Vioux, A. *J. Chem. Soc., Chem. Commun.* **1976**, 175; *J. Chem. Res., Synop.* **1977**, 168; *J. Chem. Res., Minipr.* **1977**, 1939.

[15] Colomer, E.; Corriu, R. J. P.; Vioux, A. *Inorg. Chem.* **1979**, *18*, 695.

[16] Colomer, E.; Corriu, R. J. P.; Marzin, C.; Vioux, A. *Inorg. Chem.* **1982**, *21*, 368.

[17] Schubert, U.; Ackermann, K. *J. Am. Chem. Soc.* **1982**, *104*, 7378.

[18] Cerveau, G.; Colomer, E.; Corriu, R.; Douglas, W. E. *J. Chem. Soc., Chem. Commun.* **1975**, 410; *J. Organomet. Chem.* **1977**, *135*, 373.

[19] Corriu, R. J. P.; Guerin, C. *J. Organomet. Chem.* **1980**, *198*, 232; *Adv. Organomet. Chem.* **1982**, *20*, 265.

[20] Sommer, L. H. "Stereochemistry, Mechanism and Silicon"; McGraw-Hill; New York, 1965; *Adv. Chem. Ser.*, p 104.

[21] Corriu, R. J. P.; Moreau, J. J. E. *J. Organomet. Chem.* **1976**, *114*, 135.

[22] Sommer, L. H.; Lyons, J. E. *J. Am. Chem. Soc.* **1969**, *91*, 7061.

[23] Johnson, O. H.; Harris, D. M. *J. Am. Chem. Soc.* **1950**, *72*, 5564.

[24] Gilman, H.; Gerow, C. W. *J. Am. Chem. Soc.* **1956**, *78*, 5435.

[25] Brook, A. G.; Peddle, G. J. D. *J. Am. Chem. Soc.* **1963**, *85*, 1869. Brook, A. G. *Ibid.* **1963**, *85*, 3051.

Table I. Summary of Crystal Data, Intensity Collection, and Refinement

| | |
|---|---|
| formula | $C_{25}H_{23}MnO_2Si$ |
| cryst system | orthorhombic |
| space group | $P2_12_12_1$ |
| $a$, Å | 8.7464 (57) |
| $b$, Å | 31.187 (17) |
| $c$, Å | 7.8143 (35) |
| vol, Å$^3$ | 2131.6 |
| mol wt | 438.5 |
| $Z$ | 4 |
| $d_{calcd}$, g cm$^{-3}$ | 1.366 |
| $d_{measd}$, g cm$^{-3}$ | 1.33 (1) |
| cryst size, mm$^3$ | 0.27 × 0.25 × 0.15 |
| cryst color | light yellow |
| recrystn solv | toluene/hexane |
| mp, °C | 80-81 |
| method of data collectn | moving cryst-moving counter |
| radiatn (graphite monochromated) | Mo K$\alpha$ |
| $\mu$, cm$^{-1}$ | 6.5 |
| 2$\theta$ limits, deg | 4-44 |
| no. of unique reflctns | 1564 |
| no. of obsd reflctns | 721 |
| final no. of variables | 126 |
| $R_F$ | 0.075 |
| $R_{wF}$ | 0.098 |
| error of fit | 1.88 |

chemical reactions were performed with a 100-W Hanovia medium-pressure mercury lamp. Melting points were taken under vacuum and are uncorrected. IR spectra were recorded in a Perkin-Elmer 298 spectrophotometer. NMR spectra were recorded on a Varian EM 390 or EM 360 spectrograph (chemical shifts $\delta$ are relative to $Me_4Si$).

**Crystal Structure of (−)-($\eta^5$-$CH_3C_5H_4$)($CO_2$)(MePh-1-NpSi*)(H)Mn (1). Crystal Preparation.** Crystals of complex 1 were grown by slow cooling down to −20 °C of a toluene–hexane solution in a nitrogen atmosphere. Yellow platelike blocks were obtained. Preliminary Weissenberg photography established an orthorhombic unit cell with space group $P22_12_1$ or $P2_12_12_1$. A small block cut from a plate was sealed inside a Lindeman glass capillary with the [100] direction parallel to the $\Phi$ axis of the diffractometer.

**X-ray Data Collection.** Data were collected on a CAD-4 automated diffractometer with graphite-monochromatized Mo K$\alpha$ radiation ($\lambda$ = 0.71069 Å). The goniometer head was cooled to −30 °C to prevent the decomposition of the crystal. Lattice constants (Table I) came from a least-squares refinement of 23 reflections obtained at medium and high angles. The intensities of three standard reflections were monitored after intervals of 60 min. No significant change in these intensities occurred during data collection. The observation of the systematic absence $h00$ ($h = 2n + 1$) showed unambiguously the space group to be $P2_12_12_1$. The structure amplitudes were obtained after the usual Lorentz and polarization reduction No absorption corrections were applied. Only the reflections having $\sigma(I)/I < 0.3$ were considered to be observed.

**Structure Determination and Refinement.** The Mn and Si coordinates were given by direct methods (1980 version of the MULTAN program). A Fourier map phased on these atoms revealed the methyl and carbonyl groups and 10 carbon atoms from the naphthyl, phenyl, and cyclopentadienyl groups. The remaining atoms were located after a cycle of least-squares refinement and a difference Fourier synthesis. The atomic scattering factors were taken from ref 28. Two cycles of refinement decreased the $R$ factor to 0.107.

Table II. Fractional Atomic Coordinates (×10$^4$) and Thermal Parameters (Å$^2$)

| atom | $x$ | $y$ | $z$ | $B$ |
|---|---|---|---|---|
| Mn | 4376 (4) | 4222 (1) | −541 (6) | $a$ |
| Si | 2180 (7) | 3735 (2) | −861 (10) | $a$ |
| O(1) | 1934 (21) | 4868 (5) | −416 (26) | 4.9 (4) |
| O(2) | 5384 (23) | 4524 (6) | −3880 (23) | 4.8 (4) |
| C(1) | 2896 (27) | 4607 (7) | −423 (35) | 2.7 (5) |
| C(2) | 4972 (26) | 4419 (7) | −2538 (33) | 2.5 (5) |
| Cp(1) | 5450 (32) | 4517 (8) | 1604 (31) | 3.0 (5) |
| Cp(2) | 4656 (34) | 4157 (10) | 2111 (33) | 4.4 (7) |
| Cp(3) | 5094 (32) | 3763 (10) | 1531 (35) | 4.5 (7) |
| Cp(4) | 6357 (34) | 3900 (9) | 272 (40) | 5.0 (7) |
| Cp(5) | 6603 (26) | 4354 (7) | 416 (36) | 3.2 (5) |
| Cp(6) | 7812 (32) | 4610 (8) | −461 (44) | 4.8 (6) |
| C(10) | 904 (26) | 3862 (7) | −2701 (28) | 1.8 (5) |
| C(11) | 1020 (25) | 4190 (8) | −3789 (28) | 2.8 (5) |
| C(12) | −45 (26) | 4323 (7) | −5047 (29) | 3.0 (6) |
| C(13) | −1343 (29) | 4079 (7) | −5212 (32) | 3.3 (6) |
| C(14) | −1545 (32) | 3715 (9) | −4195 (39) | 4.6 (6) |
| C(15) | −386 (30) | 3593 (8) | −2876 (33) | 3.2 (6) |
| C(20) | 2613 (26) | 3137 (7) | −1007 (31) | 2.7 (5) |
| C(21) | 2106 (31) | 2877 (8) | 335 (37) | 4.1 (6) |
| C(22) | 2330 (33) | 2415 (8) | 305 (40) | 4.9 (7) |
| C(23) | 2967 (31) | 2236 (8) | −1051 (35) | 3.8 (6) |
| C(24) | 4294 (29) | 2288 (7) | −3823 (29) | 2.7 (5) |
| C(25) | 4828 (29) | 2498 (9) | −5156 (34) | 3.8 (6) |
| C(26) | 4652 (30) | 2963 (7) | −5186 (32) | 3.8 (6) |
| C(27) | 3887 (27) | 3171 (8) | −3839 (32) | 3.2 (6) |
| C(28) | 3345 (27) | 2927 (7) | −2433 (32) | 2.3 (5) |
| C(29) | 3554 (27) | 2468 (7) | −2457 (30) | 2.2 (5) |
| C(30) | 1048 (29) | 3809 (8) | 1113 (32) | 3.3 (6) |

[a] The anisotropic thermal parameters (×10$^4$) for manganese and silicon are as follows: Mn, 25 (4), 8.0 (5), 168 (7), 2 (1), −23 (7), −2 (2); Si, 43 (8), 7.4 (8), 154 (16), 0 (2), 5 (12), −5 (4). The thermal elipsoid is given by $\exp[-(\beta_{11}h^2 + \beta_{22}k^2 + \beta_{33}l^2 + 2\beta_{12}hk + 2\beta_{13}hl + 2\beta_{23}kl)]$.

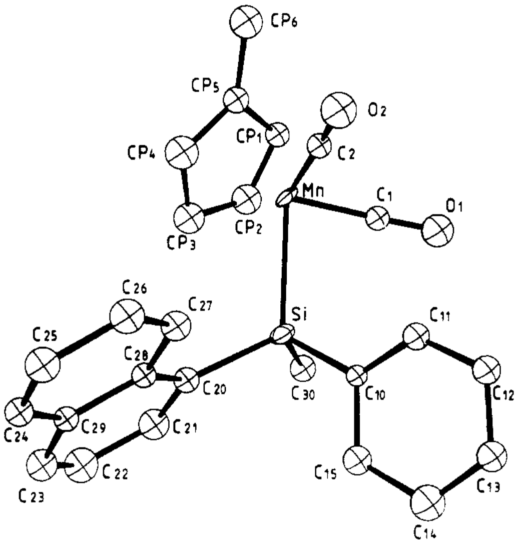

**Figure 1.** ORTEP drawing of complex 1 with the numbering of the atoms. The ellipsoids enclose 30% of the electron density.

At this stage the absolute configuration was determined. The manganese and silicon atoms were then given anisotropic thermal parameters. The real and imaginary parts of Mn and Si scattering factors[29] were introduced in calculations. The structure factors were computed for both enantiomers and the least-squares refinements were carried out separately. After three cycles of refinement, the agreement indices were $R^+ = 0.081$, $R_w^+ = 0.106$ and $R^- = 0.075$, $R_w^- = 0.098$. Their ratio (1.080 and 1.082) indicates the second model is preferred at a significant level of greater than 99.5%.[30] Thus this model was chosen for the structure of the molecule: the absolute configuration at silicon is $S$.

During the last cycle of least-squares refinement the largest shift-to-error ratio was 0.28. A final difference Fourier map revealed peaks no larger than 0.48 e Å$^{-3}$. In view of the low number

---

(26) Brook, A. G.; Peddle, G. J. D. *J. Am. Chem. Soc.* **1963**, *85*, 2338.

(27) Poskozim, P. S.; Stone, A. L. *J. Inorg. Nucl. Chem.* **1970**, *32*, 1391.

(28) Doyle, P. A.; Turner, P. S. *Acta Crystallogr., Sect. A* **1968**, *A24*, 390.

(29) "International Tables for X-ray Crystallography"; Kynoch Press. Birmingham, 1968; Vol. 3, p 215.

(30) Hamilton, W. C. *Acta Crystallogr.* **1965**, *18*, 502.

**Table III. Bond Lengths (Å) Measured for Complex 1**

| | | | |
|---|---|---|---|
| Mn–Si | 2.461 (7) | C(10)–C(11) | 1.34 (3) |
| Mn–C(1) | 1.77 (2) | C(11)–C(12) | 1.42 (3) |
| Mn–C(2) | 1.76 (3) | C(12)–C(13) | 1.37 (3) |
| Mn–CP(1) | 2.13 (3) | C(13)–C(14) | 1.40 (4) |
| Mn–CP(2) | 2.10 (3) | C(14)–C(15) | 1.49 (4) |
| Mn–CP(3) | 2.14 (3) | C(15)–C(10) | 1.41 (3) |
| Mn–CP(4) | 2.10 (3) | | |
| Mn–CP(5) | 2.13 (3) | C(20)–C(21) | 1.40 (4) |
| | | C(21)–C(22) | 1.45 (4) |
| Si–C(10) | 1.86 (2) | C(22)–C(23) | 1.32 (4) |
| Si–C(20) | 1.91 (3) | C(23)–C(29) | 1.41 (4) |
| Si–C(30) | 1.85 (3) | C(29)–C(24) | 1.37 (3) |
| | | C(24)–C(25) | 1.32 (4) |
| C(1)–O(1) | 1.17 (3) | C(25)–C(26) | 1.46 (4) |
| C(2)–O(2) | 1.16 (3) | C(26)–C(27) | 1.41 (3) |
| | | C(27)–C(28) | 1.42 (3) |
| CP(1)–CP(2) | 1.38 (4) | C(28)–C(20) | 1.44 (3) |
| CP(2)–CP(3) | 1.42 (4) | C(28)–C(29) | 1.45 (3) |
| CP(3)–CP(4) | 1.44 (4) | | |
| CP(4)–CP(5) | 1.44 (4) | | |
| CP(5)–CP(1) | 1.46 (4) | | |
| CP(5)–CP(6) | 1.49 (4) | | |

of observed reflections, no attempt was made to assign anisotropic thermal parameters to carbon and oxygen atoms; the quality of the data prevented also undertaking accurate determination of the hydrogen atoms.

The final atomic coordinates with the associated thermal parameters are listed in Table II. The labeling scheme is given on Figure 1. Individual bond lengths are listed in Table III and important bond angles in Table IV. A list of observed and calculated structure factors (Table VII) is available as supplementary material.

**$(\eta^5\text{-}CH_3C_5H_4)(CO)_2(Ph_3Ge)(H)Mn$ (2).** A solution of $Ph_3GeH$ (915 mg, 3 mmol) and $(\eta^5\text{-}CH_3C_5H_4)(CO)_3Mn$ (872 mg, 4 mmol) in 100 mL of THF was irradiated overnight. The solvent was removed under vacuum. The residue was dissolved in hexane and filtered. The solution was concentrated to ca. 20 mL and then allowed to crystallize at −20 °C. Yellow crystals of 2 (465 mg, 31%), were thus obtained: mp 109–110 °C; IR ($CH_2Cl_2$) $\nu$(CO) 1965 (s), 1910 (m) cm$^{-1}$; $^1H$ NMR ($C_6D_6$) $\delta$ 7.66–7.13 (aromatic, 15 H, m), 3.93 ($C_5H_4$, 4 H, s), 1.41 ($CH_3Cp$, 3 H, s), −9.08 (MnH, 1 H, s). Anal. Calcd for $C_{26}H_{23}GeMnO_2$: C, 63.08; H, 4.65. Found: C, 63.09; H, 4.69.

**$[(\eta^5\text{-}CH_3C_5H_4)(CO)_2(Ph_3Ge)Mn]Et_4N$.** A solution of $Ph_3GeLi$ (from 3.05 g, 10 mmol, of $Ph_3GeH$ and 10 mmol of *n*-BuLi)[24] in 20 mL of ether was added dropwise to a solution of $(\eta^5\text{-}CH_3C_5H_4)(CO)_3Mn$ (2.2 g, 10 mmol) in 50 mL of ether. The mixture was refluxed overnight, and a yellow precipitate was obtained. The solvent was pumped off. The residue was dissolved in 30 mL of $CH_2Cl_2$ and treated with a solution of $Et_4NCl$ (1.64 g, 10 mmol) in 20 mL of $CH_2Cl_2$. The solution was filtered through a fritted funnel (G4) and then evaporated. The residue was taken up in THF, and the excess $Et_4NCl$ was filtered. The solvent was pumped off again. Crystallization from $CH_2Cl_2$/hexane (50/50) at −20 °C afforded yellow crystals of $[(\eta^5\text{-}CH_3C_5H_4)(CO)_2(Ph_3Ge)Mn]Et_4N$ (4.1 g, 66%): mp 174–175 °C; IR ($CH_2Cl_2$) $\nu$(CO) 1855 (s), 1775 (m) cm$^{-1}$; $^1H$ NMR ($CD_2Cl_2$) $\delta$ 7.57–7.17 (aromatic, 15 H, m), 4.17, 3.97 ($C_5H_4$, 4 H, br s), 2.70 ($CH_2N$, 8 H, q), 1.84 ($CH_3Cp$, 3 H, s), 0.94 ($CH_3C$, 12 H, t). Anal. Calcd for $C_{34}H_{42}GeMnNO_2$: C, 65.43; H, 6.74; N, 2.25. Found: C, 65.20; H, 6.71; N, 2.11.

**Reaction of $[(\eta^5\text{-}CH_3C_5H_4)(CO)_2(Ph_3Ge)Mn]Et_4N$ with HCl.** A 0.35 N solution of HCl in THF was prepared by bubbling dry hydrogen chloride into the solvent; 15 mL of this solution was added dropwise to 20 mL of a solution of $[(\eta^5\text{-}CH_3C_5H_4)(CO)_2(Ph_3Ge)Mn]Et_4N$ (3.1 g, 5 mmol) in THF. The reaction was monitored by IR spectroscopy until disappearance of the CO absorptions corresponding to the anion. The solvent was removed under vacuum and the residue taken up in toluene. The solution was filtered and concentrated to ca. 10 mL. Addition of hexane (ca. 20 mL) and standing at −20 °C afforded yellow crystals of $(\eta^5\text{-}CH_3C_5H_4)(CO)_2(Ph_3Ge)(H)Mn$ (1.43 g 57%). The melting point and IR and NMR spectra were identical with those of complex 2 (vide supra).

**$[(\eta^5\text{-}CH_3C_5H_4)(CO)_2(Cl_3Ge)Mn]Me_4N$.** A solution of $Me_4NGeCl_3$ (750 mg, 3 mmol) and $(\eta^5\text{-}CH_3C_5H_4)(CO)_3Mn$ (660 mg, 3 mmol) in 100 mL of THF was irradiated for 24 h. The mixture was filtered and then evaporated under vacuum. The residue was dissolved in the minimum amount of $CH_2Cl_2$. Addition of $Et_2O$ and standing at −20 °C afforded yellow crystals of $[(\eta^5\text{-}CH_3C_5H_4)(CO)_2(Cl_3Ge)Mn]Me_4N$ (730 mg, 55%): mp 78–79 °C; IR ($CH_2Cl_2$) $\nu$ (CO) 1920 (s), 1850 (s) cm$^{-1}$; $^1H$ NMR ($CD_2Cl_2$) $\delta$ 4.26 ($C_5H_4$, 4 H, s), 3.16 ($CH_3N$, 12 H, br s), 1.80 ($CH_3Cp$, 3 H, s). Anal. Calcd for $C_{12}H_{19}Cl_3GeMnO_2$: C, 32.50; H, 4.29; Cl, 24.01; N, 3.16. Found: C, 32.25; H, 4.29; Cl, 24.50; N, 3.14.

**Reaction of $[(\eta^5\text{-}CH_3C_5H_4)(CO)_2(Cl_3Ge)Mn]Me_4N$ with $H_3PO_4$.** A solution of $[(\eta^5\text{-}CH_3C_5H_4)(CO)_2(Cl_3Ge)Mn]Me_4N$ (890 mg, 2 mmol) in 20 mL of $CH_2Cl_2$ was stirred with 2 mL of phosphoric acid (85%) at room temperature for 3 h. After the mixture was allowed to settle, the $CH_2Cl_2$ layer was decanted. The IR spectrum of the solution showed $\nu$(CO) absorptions at 2040 (s) and 1980 (m) cm$^{-1}$ assigned to *cis*-$(\eta^5\text{-}CH_3C_5H_4)(CO)_2(Cl_3Ge)(H)Mn$. Unfortunately all of our attempts to crystallize the complex were unsuccessful.

**$[(\eta^5\text{-}CH_3C_5H_4)(CO)_2(1\text{-}NpPhMeGe)Mn]Et_4N$ (3).** A solution of $(\eta^5\text{-}CH_3C_5H_4)(CO)_3Mn$ (2.2 g, 10 mmol) in 40 mL of ether was treated by a solution of 1-NpPhMeGeLi (from 2.9 g, 10 mmol, of 1-NpPhMeGeH[26] in 20 mL of ether (see experimental of $[(\eta^5\text{-}CH_3C_5H_4)(CO)_2(Ph_3Ge)Mn]Et_4N$ above). Racemic $[(\eta^5\text{-}CH_3C_5H_4)(CO)_2(1\text{-}NpPhMeGe)Mn]Et_4N$ was obtained in a 33% yield: mp 53–55 °C. IR ($CH_2Cl_2$) $\nu$(CO) 1850 (s), 1775 (s) cm$^{-1}$; $^1H$ NMR ($CD_2Cl_2$) $\delta$ 8.67, 7.63–7.20 (aromatic, 12 H, m), 4.04, 3.87 ($C_5H_4$, 4 H, br s), 2.90 ($CH_2$ N, 8 H, q), 1.80 ($CH_3Cp$, 3 H, s), 1.10 ($CH_3C$, 12 H, t), 0.70 ($CH_3Ge$, 3 H, s). Anal. Calcd for $C_{34}H_{44}GeMnNO_2Cl_2$ (crystallizes with one molecule of $CH_2Cl_2$): C, 58.57; H, 6.32; N, 2.01; Cl, 10.19. Found: C, 58.59; H, 6.51; N, 2.16; Cl, 9.96. The optically active (*S*)-$[(\eta^5\text{-}CH_3C_5H_4)(CO)_2(1\text{-}NpPhMeGe^*)Mn]Et_4N$ was obtained in the same way from the optically active germyllithium (from 1.46 g, 5 mmol, of (*R*)-1-NpPhMeGeH, $[\alpha]^{25}_D$ (cyclohexane) +23° in a 25% yield: mp 59–60 °C; $[\alpha]^{25}_D$ −3.9° (*c* 6.4, $CH_2Cl_2$).

**Reaction of (*S*)-(−)-$[(\eta^5\text{-}CH_3C_5H_4)(CO)_2(1\text{-}NpPhMeGe^*)Mn]Et_4N$ (3) with HCl.** A solution of HCl in THF (10 mL, 0.31 N) was added dropwise to a solution of 3 (1.22 g, 2 mmol) in THF (30 mL). The reaction was followed by IR spectroscopy in order to check the disappearance of the $\nu$(CO) absorptions due to the anion and the appearance of new ones corresponding to *cis*-$(\eta^5\text{-}CH_3C_5H_4)(CO)_2(1\text{-}NpPhMeGe^*)(H)Mn$ (4) (1960 (s), 1900 (m) cm$^{-1}$). The usual workup did not afford any crystals.

No suitable $^1H$ NMR spectrum could be obtained since this kind of complexes need careful crystallizations to free them from paramagnetic impurities (cf. ref 9 and 16). The structure of 4 is attributed by comparison to the reaction of the parent inactive

**Table IV. Selected Bond Angles (deg) Measured for Complex 1**

| | | | | | |
|---|---|---|---|---|---|
| Si–Mn–C(1) | 81.6 (8) | Mn–Si–C(10) | 114.5 (8) | CP(5)–CP(1)–CP(2) | 104.4 (22) |
| Si–Mn–C(2) | 111.0 (8) | Mn–Si–C(20) | 117.0 (7) | CP(1)–CP(2)–CP(3) | 116.3 (25) |
| Si–Mn–CP[a] | 118.6 | Mn–Si–C(30) | 104.9 (8) | CP(2)–CP(3)–CP(4) | 101.4 (25) |
| C(1)–Mn–CP | 121.7 | C(10)–Si–C(20) | 106.3 (10) | CP(3)–CP(4)–CP(5) | 111.1 (25) |
| C(2)–Mn–CP | 122.7 | C(10)–Si–C(30) | 107.3 (11) | CP(4)–CP(5)–CP(1) | 106.8 (22) |
| C(1)–Mn–C(2) | 91.4 (11) | C(20)–Si–C(30) | 106.2 (11) | CP(4)–CP(5)–CP(6) | 126.6 (24) |
| Mn–C(1)–O(1) | 177.1 (24) | Si–C(10)–C(11) | 127.5 (18) | CP(1)–CP(5)–CP(6) | 126.6 (21) |
| Mn–C(1)–O(2) | 175.8 (20) | Si–C(10)–C(15) | 115.3 (17) | Si–C(20)–C(21) | 117.4 (18) |
| | | C(11)–C(10)–C(15) | 117.0 (21) | Si–C(20)–C(28) | 125.3 (17) |
| | | | | C(21)–C(20)–C(28) | 117.2 (21) |

[a] CP is the calculated center of the cyclopentadienyl ring with coordinates 0.5632, 0.4138, and 0.1147.

Table V. Deprotonation Reactions on Complex 2

| reagent | solv | $\nu$(CO), cm$^{-1}$ (due to the anion) |
|---|---|---|
| $Et_4NCl$ | $CH_2Cl_2$ | 1855, 1775 |
| $Et_3N$ | $C_6H_{14}$ | 1850, 1780, 1730 |
| MeLi | $Et_2O$ | 1830, 1780, 1750 |
| $LiAlH_4$[a] | $Et_2O$ | 1830, 1780, 1750 |
| NaH[a] | THF | 1830, 1780, 1750 |

[a] Excess.

Table VI. Cleavage Reactions on Complex 2

| reagent | solv | time | final product |
|---|---|---|---|
| $CH_3OH$ | $Et_2O$ | 8 days | $Ph_3GeOCH_3$ |
| $H_2O$ | $Et_2O$ | 8 days | $Ph_3GeOH$ |
| $Cl_2$ | $C_6H_6$ | 2 h | $Ph_3GeCl$ |
| $CCl_4$ | $CCl_4$ | 48 h | $Ph_3GeCl$ |

salt, which gives 2 by protonation, and in light of the reaction of 4 with $PPh_3$ (vide infra).

**Reaction of 2 and 4 with $PPh_3$.** A solution of 2 (495 mg, 1 mmol) and $PPh_3$ (262 mg, 1 mmol) in 5 mL of toluene was stirred at room temperature for 6 days. The reaction was followed by IR spectroscopy until disappearance of the $\nu$(CO) absorptions due to complex 2 was complete. The mixture was chromatographed on alumina. Elution with hexane afforded a colorless band corresponding to $Ph_3GeH$ (270 mg, 90%). Then elution with toluene afforded a yellow band corresponding to $(\eta^5\text{-}CH_3C_5H_4)(CO)_2PPh_3Mn$ ($\nu$(CO) 1928, 1860 cm$^{-1}$) that was compared to an authentic sample.[31]

In the same way the optically active $(\eta^5\text{-}CH_3C_5H_4)(CO)_2$(1-NpPhMeGe*)(H)Mn (from (*R*)-1-NpPhMeGe*H $[\alpha]^{25}_D$ + 23°, vide supra) was treated by $PPh_3$. The optically active (*R*)-1-$C_{10}H_7$PhMeGe*H ($[\alpha]^{25}_D$ + 18.7°) was isolated. The overall stereospecificity was 91% retention.

**Deprotonation Reactions on 2.** Complex 2 was treated in the appropriate solvent by the reagent (Table V) at room temperature. The reactions, followed by IR spectroscopy, were complete after ca. 1 h. In each case the anion was isolated in a ca. 90% yield as the tetraethylammonium salt (vide supra).

**Cleavage Reactions on 2.** Complex 2 was treated by an excess of reagent (an equimolar amount of $Cl_2$ was used) in the appropriate solvent. The reactions were followed by IR spectroscopy until disappearance of the $\nu$(CO) absorptions of the starting material. The absence of $Ph_3GeH$ was proved by thin-layer chromatography. Table VI shows the final products obtained. $Ph_3GeOMe$ was isolated by crystallization from hexane at −20 °C in a 75% yield and identified by NMR and IR spectroscopies. In the other cases the crude final product was reduced with $LiAlH_4$ in $Et_2O$ at room temperature (the reduction of $Ph_3GeOH$ takes place in refluxing $Bu_2O$). The usual workup afforded $Ph_3GeH$ in good yields (~90%).

## Results and Discussion

**Description of the Structure of (−)-$(\eta^5\text{-}CH_3C_5H_4)(CO)_2(1\text{-}C_{10}H_7PhMeSi)(H)Mn$ (1).** Figure 1 gives a perspective view of the molecule with the numbering of the atoms. The cyclopentadienyl ring shows no unusual features: the carbon atom CP(6) is coplanar with the ring as shown by the angles around carbon CP(5) (Table IV) and lies away from the naphthyl group. A neutron diffraction study[17] on a fluorinated silicon–manganese complex, $(\eta^5\text{-}CH_3C_5H_4)(CO)_2(Ph_2FSi)(H)Mn$ revealed metal–carbonyl distances of 1.796 and 1.782 (3) Å. Here, the average of the manganese–carbonyl distances (1.765 (2) Å) is slightly shorter and comparable to the value reported for carbonyls trans to chlorine or phosphorus atoms in the complex *cis*-$Cl(PPh_3)Mn(CO)_4$:[32] 1.752 Å. This is near the values (average: 1.759 Å) measured for the germyl-manganese complex *cis*-(MePh-1-NpGe)(MeEtOC)$(CO)_4$Mn.[33] The geometry around silicon (Figure 2) is tetrahedral with minor distorsions apparently due to repulsion between the phenyl and naphthyl groups and the methylcyclopentadienylmanganese dicarbonyl moeity (Mn–Si–C(10) = 114.5 (8)°; Mn–Si–C(20) = 117.0 (7)°). However, analogous values (115.8 (1), 117.3 (1)°) are reported for the complex of ref 17 where the Mn–H···Si interaction is clearly established. In the present work the quality of the diffraction data was not sufficient to locate the hydrogen atom and such an interaction can only be supposed as probable.

Scheme VII

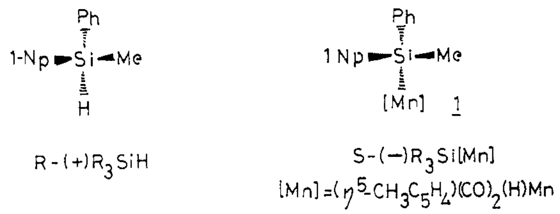

Scheme VIII

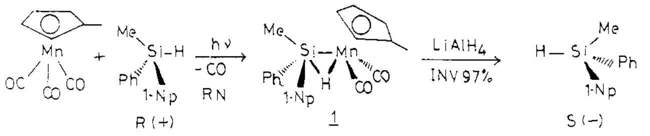

Scheme IX

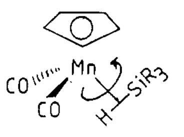

Scheme X

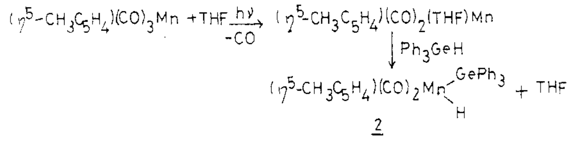

Scheme XI

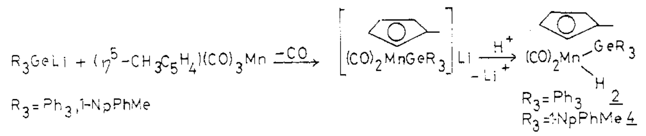

**Absolute Configuration of Complex 1.** The X-ray diffraction analysis of complex 1 shows that the absolute configuration at silicon is S. Thus, the relative configurations of (*S*)-1 and (*R*)-(+)-MePh-1-NpSiH[34] are the same (Scheme VII). This means that the silane has reacted with retention of configuration and confirms the Walden cycles that we has assumed in a previous work,[14] for example, the one shown in Scheme VIII.

In the crystalline state, the manganese atom appears to be chiral since the Si–Mn–CO angles are very different, 81.6 and 111.0°, a feature already reported[17] (78.1 and 115.2°. In contrast, in solution, the Si–H moiety behaves as a single ligand (cf. Introduction) and complex 1 can be considered as fluxional. In the solid state the most favored rotational isomer (not diastereoisomer) is isolated (Scheme IX).

---

[31] Nyholm, R. S.; Sandhu, S. S.; Stiddard, M. H. B. *J. Chem. Soc.* **1963**, 5916.

[32] Vahrenkamp, H. *Chem. Ber.* **1971**, *104*, 449.

[33] Carré, F.; Cerveau, G.; Colomer, E.; Corriu, R. J. P. *J. Organomet. Chem.* **1982**, *229*, 257.

[34] Okaya, Y.; Ashida, T. *Acta Crystallogr.* **1966**, *20*, 461.

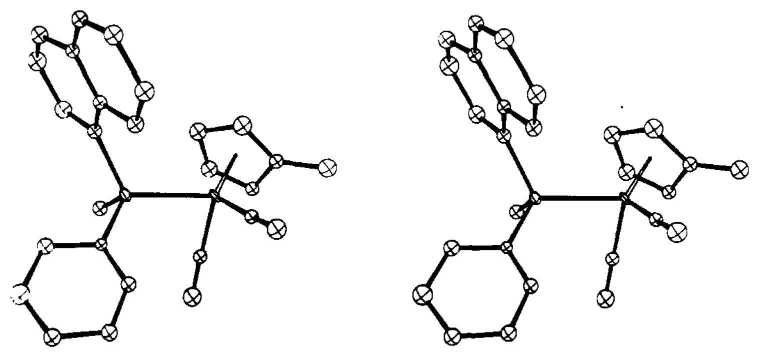

**Figure 2.** Stereoscopic view of the molecule with 20% probability ellipsoids.

Scheme XII

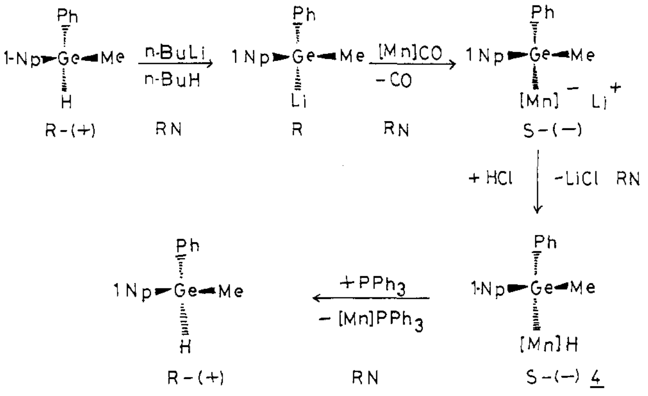

**Synthesis of Germylmanganese Complexes.** Two routes can lead to the related germyl complexes. (A) The direct route corresponds to the oxidative addition of a Ge–H bond to the transition-metal atom. This process is often inefficient as reported by Graham et al. in the case of rhenium[13] or iron[35] although the silyl analogues were synthesized in this way. Nevertheless we succeeded in preparing $(\eta^5\text{-}CH_3C_5H_4)(CO)_2(GePh_3)(H)Mn$ (2) by irradiating a solution of $Ph_3GeH$ and $(\eta^5\text{-}CH_3C_5H_4)(CO)_3Mn$ in tetrahydrofuran (Scheme X). We assume that THF behaves as a readily displaced ligand in the intermediate $(\eta^5\text{-}CH_3C_5H_4)(CO)_2(THF)Mn$.[36] (B) An alternative pathway is shown in Scheme XI. The germyl anions are known to behave as Lewis bases toward ($\eta^5$-methylcyclopentadienyl)tricarbonylmanganese affording the manganate anions $[(\eta^5\text{-}CH_3C_5H_4)(CO)_2MnGeR_3]^-$ (R = halide, organic radical). Carbonyl substitution occurs photochemically in THF solution with $Cl_3Ge^-$[37] and thermally with $R_3Ge^-$, prepared by reaction of *n*-BuLi on $R_3GeH$ ($R_3$ = $Ph_3$, MePh-1-Np).[38,39]

(Organogermyl) lithium 1-NpPhMeGe*Li prepared from optically active (*R*)-(+)-1-NpPhMeGe*H was reported to be optically stable.[26,40] Its use leads to the optically active anion $[(\eta^5\text{-}CH_3C_5H_4)(CO)_2Mn(Ge^*MePh\text{-}1\text{-}Np)]^-$ which is isolated as the tetraethylammonium salt 3 ($[\alpha]^{25}_D$ −3.9° in $CH_2Cl_2$). Protonation of 3 affords the related hydride 4 $(\eta^5\text{-}CH_3C_5H_4)(CO)_2Mn(H)(Ge^*MePhNp)$ that unfortunately could not be isolated by crystallization.

Scheme XIII

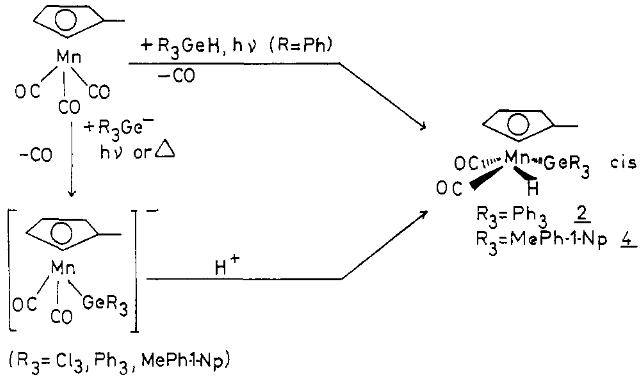

Scheme XIV

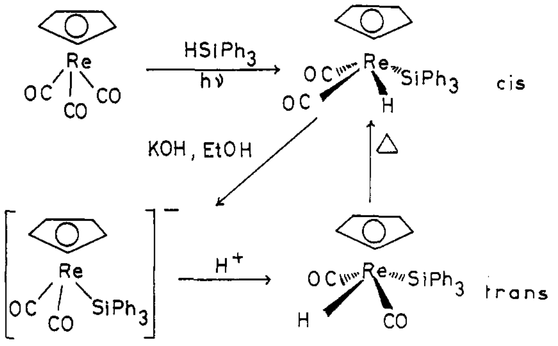

The configuration around the germanium atom in 3 can be assumed to be the same as in the starting germane, since optically active germyl lithium is always known to react with retention of configuration either with organic substrates[40] or with transition-metal complexes.[41,42] This assumption is supported by the Walden cycle represented in Scheme XII: protonation of 3 takes place with retention of configuration since it does not involve the chiral center; on the other hand reaction of $PPh_3$ on the neutral complex 4 involves the reductive elimination of (*R*)-(+)-1-NpPhMeGe*H.

**Structure of the Germylmanganese Hydrides.** Independent of the method used to prepare the germylmanganese hydrides only the cis isomers are obtained (Scheme XIII). We reported previously the same observation for the silylmanganese hydrides.[16] This assignment of configuration is based on the relative intensities of the two carbonyl stretching bands in the IR spectrum, namely, the higher frequency (symmetric) stretching band is slightly more intense than the lower. A similar assign-

---

(35) Isaacs, E. E.; Graham, W. A. G. *J. Organomet. Chem.* **1975**, *85*, 237.

(36) Strohmeier, W.; van Hobe, D.; Schönauer, G.; Laporte H. *Z. Naturforsch., B: Anorg. Chem., Org. Chem., Biochem., Biophys., Biol.* **1962**, *17B*, 502.

(37) Ruff, J. K. *Inorg. Chem.* **1971**, *10*, 409.

(38) Colomer, E.; Corriu, R. J. P. *J. Chem. Soc., Chem. Commun.* **1978**, 435.

(39) Colomer, E.; Corriu, R. J. P.; Vioux, A. *Angew. Chem., Int. Ed. Engl.* **1981**, *20*, 476.

(40) Carré, F.; Corriu, R. J. P. *J. Organomet. Chem.* **1974**, *65*, 349 and references therein.

(41) Carré, F.; Cerveau, G.; Colomer E.; Corriu, R. J. P. *J. Organomet. Chem.* **1982**, *229*, 257.

(42) Cerveau, G.; Colomer, E.; Corey, E. R.; Corriu, R. J. P.; Vioux, A., to be submitted for publication in *Organometallics*.

Scheme XV

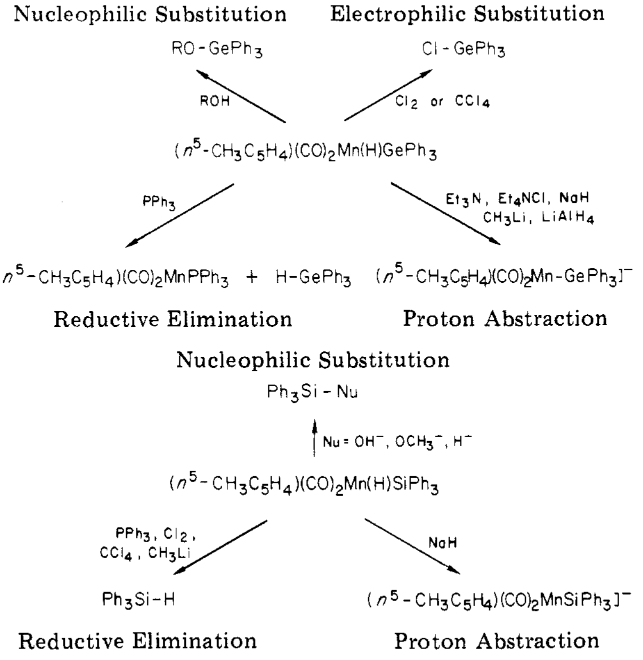

ment has been proposed[9,13] for other silylmanganese hydrides and confirmed by X-ray[10] and neutron diffraction studies.[17]

The absence of the trans form may be related to an attractive interaction between hydrogen and germanium (or silicon) that stabilizes the lateral geometry via a three-center bonding. Indeed, the alkylation of the salts gives only the trans isomers, independent of whether the anion has been generated; the same fact was observed for the case of the parent silylmanganese anions.[16] The alkylated complexes are much more chemically and thermodynamicly stable than the hydrides and are not isomerized to the cis isomers.

It is noteworthy that in the case of the related rhenium complex $(\eta^5\text{-}C_5H_5)(CO)_2(Ph_3Si)(H)Re$, both cis and trans isomers are obtained. Nevertheless the latter isomerizes thermally to the former in solution (Scheme XIV).[13]

**Chemical Behavior of the Germylmanganese Complexes.** Scheme XV summarizes the chemical behavior of the germyl complex **2**, compared to that of the silyl analogue.

The different reactions may be classified into three types: (i) elimination reaction, (ii) cleavage of the Mn–Ge bond, and (iii) formation of anions by abstraction of $H^+$.

**(i) Elimination Reaction.** Compound **2** undergoes elimination of germane when treated with triphenylphosphine in solution at room temperature. The same reaction was reported for related silylmanganese and silylrhenium complexes.[9,13] Moreover Graham reported that the elimination rate was much slower for the latter than for the former. However we did not observe any noteworthy change between the elimination rates of silanes and germanes.

**(ii) Cleavage of the Mn–Ge Bond.** Nucleophiles such as water or methanol and electrophiles such as chlorine or $CCl_4$ cleave and the Mn–Ge bond, affording germanol or methoxygermane for the former reagents and chlorogermane for the latter. It is interesting to compare this behavior to that of the silyl analogue since a stoichiometric amount of $Cl_2$, surprisingly, led to elimination of silane (without chlorination of the Si–H function).[14] This indicates that these reactions probably occur on the 18-electron complex, since reaction on the 16-electron species could lead to chlorination of the Si–H.

**(iii) Proton Abstraction.** The deprotonation of the germylmanganese hydride **2** takes place with strong bases (NaH, $LiAlH_4$, $CH_3Li$), independent of their nucleophilicity, weak bases ($Et_3N$), and even $Et_4NCl$. In this case HCl is displaced, showing that the germylmanganese hydride **2** is a strong acid with a $pK_a$ close to that of HCl.

## Conclusion

Comparison of the chemical properties of $(\eta^5\text{-}CH_3C_5H_4)(CO)_2Mn(H)GePh_3$ (**2**) and those of the silicon analogue[14,15] (Scheme XV) leads to the conclusion that the behavior is very similar in spite of some differences. These differences appear in the reactions with $Cl_2$ and $CCl_4$, that involve cleavage of the Mn–Ge bond instead of elimination. It is difficult to relate these differences either with a weaker ability for the elimination or to a weaker Mn–Ge bond. Nevertheless the greater acidity of the germyl complex **2** can be invoked to explain the differences shown by the reactions of **1** with $Et_3N$ or $Et_4NCl$ (no reaction with the silyl compound), MeLi (elimination of silane), and $LiAlH_4$ (nucleophilic substitution at silicon).

On the other hand, similarities appear through three main features: (i) only the cis form is obtained by protonation of the anion; (ii) elimination is easy with triphenylphosphine; (iii) group 4B elements undergo nucleophilic substitutions.

These observations are in agreement with a two-electron, three-center Mn–H–Ge interaction. Similar bonds were reported in the W–H–Si,[43] Pt–H–Si,[44] and Mn–H–C[45] triangles. However, only a neutron diffraction study could confirm this assumption in the case of Mn–H–Ge, as was seen for the Mn–H–Si bond.[17]

**Acknowledgment.** We are grateful to R. Astier and Dr. E. Philippot of the Laboratoire de Chimie Minérale – Chimie des Matériaux, ERA au CNRS N° 314, Université des Sciences et Techniques de Languedoc, for the help of data collection on a Nonius CAD-4 diffractometer.

**Registry No.** **1**, 64161-77-9; **2**, 90148-95-1; **3**, 78086-83-6; **4**, 90148-96-2; $[(\eta^5\text{-}CH_3C_5H_4)(CO)_2(Ph_3Ge)Mn]Et_4N$, 68168-06-9; $[(\eta^5\text{-}CH_3C_5H_4)(CO)_2(Cl_3Ge)Mn]Me_4N$, 90148-97-3; *cis*-$(\eta^5\text{-}CH_3C_5H_4)(CO)_2(Cl_3Ge)(H)Mn$, 90148-98-4; $Ph_3GeH$, 2816-43-5; $(\eta^5\text{-}CH_3C_5H_4)(CO)_3Mn$, 12108-13-3; $Ph_3GeLi$, 3839-32-5; $Me_4NGeCl_3$, 27121-57-9; 1-NpPhMeGeLi, 51894-87-2; (*R*)-1-$C_{10}H_7PhMeGe^*H$, 23190-27-4.

**Supplementary Material Available:** Table VII, a listing of structure factor amplitudes (7 pages). Ordering information is given on any current masthead page.

---

(43) Bennett, M. J.; Simpson, K. A. *J. Am. Chem. Soc.* **1971**, *93*, 7156.

(44) Auburn, M.; Ciriano, M.; Howard, J. A. K.; Murray, M.; Pugh, N. J.; Spencer, J. L.; Stone, F. G. A.; Woodward, P. *J. Chem. Soc., Dalton Trans.* **1980**, 659.

(45) Brookhart, M.; Lukacs, A. *J. Am. Chem. Soc.* **1983**, *2*, 649 and references therein.